Robust Beamforming Design for Intelligent Reflecting Surface Aided MISO Communication Systems

Gui Zhou, Cunhua Pan, *Member, IEEE*, Hong Ren, *Member, IEEE*, Kezhi Wang, *Member, IEEE*, Marco Di Renzo, *Fellow, IEEE*, and Arumugam Nallanathan, *Fellow, IEEE*

***Abstract*—Perfect channel state information (CSI) is challenging to obtain due to the limited signal processing capability at the intelligent reflection surface (IRS). This is the first work to study the worst-case robust beamforming design for an IRS-aided multiuser multiple-input single-output (MU-MISO) system under the assumption of imperfect CSI. We aim for minimizing the transmit power while ensuring that the achievable rate of each user meets the quality of service (QoS) requirement for all possible channel error realizations. With unit-modulus and rate constraints, this problem is non-convex. The imperfect CSI further increases the difficulty of solving this problem. By using approximation and transformation techniques, we convert the optimization problem into a squence of semidefinite program (SDP) subproblems that can be efficiently solved. Numerical results show that the proposed robust beamforming design can guarantee the required QoS targets for all the users.**

***Index Terms*—Intelligent reflecting surface (IRS), large intelligent surface (LIS), robust design, imperfect channel state information (CSI), semidefinite program (SDP).**

I. Introduction

INTELLIGENT reflecting surface (IRS) has recently been proposed as a cost-effective and energy-efficient high data rate communication technology due to the rapid development of radio frequency (RF) micro-electro-mechanical systems (MEMS) as well as the abundant applications of programmable and reconfigurable metasurfaces [1]. IRS consists of a passive array structure that is capable of adjusting, continuously or discretely and at low power consumption, the phase of each passive element on the surface [2], [3]. The benefits of IRS in enhancing the spectral and energy efficiency have been demonstrated in various system setups (e.g., [4]–[9]) by the joint design of active precoding at the base station (BS) and passive reflection beamforming at the IRS.

However, the existing contributions on IRS are based on the assumption of perfect channel state information (CSI) at the BS, which is an idealistic in IRS communications. As for the imperfect CSI, the authors of [10] studied the impact of channel errors in an uplink multiple-input single-output (MISO) system. There are three types of channels in an IRS-aided system: the **direct channel** from the BS to the user, the **indirect channel** from the BS to the IRS and the **reflection channel** from the IRS to the user. The first one can be obtained with high accuracy by using conventional channel estimation methods. The accurate CSI of the latter two, however, is challenging to obtain in practice due to the fact that the reflective elements at the IRS are passive and have limited signal processing capabilities. Fortunately, the location of the IRS is fixed and is usually installed on the building facades, ceilings, walls, etc. In this case, the **indirect channel** can be accurately estimated through calculating the angles of arrival and departure, which vary slowly. In contrast, the **reflection channel** is more challenging to acquire as the locations of users and the environmental conditions change over time.

Against this background, this letter investigates the robust active precoding and passive reflection beamforming design for an IRS-aided downlink multiple-user MISO (MU-MISO) system based on the assumption of imperfect **reflection channel**. An ellipsoid model for the reflection channel uncertainties is adopted. To the best of our knowledge, this is the first work to study the worst-case robust beamforming design problem in IRS-aided wireless systems. The contributions of this letter are as follows: 1) We minimize the transmit power of the BS through the joint design of an active precoder at the BS and a passive beamforming at the IRS while ensuring that each user's QoS target can be achieved for all possible channel error realizations. This problem is non-convex and difficult to solve due to the unit-modulus constraints and the imperfect CSI. 2) To address this problem, we propose an iterative algorithm based on approximation transformations and a convex–concave procedure (CCP). Specifically, to handle the non-convex rate expression and CSI uncertainties, we first approximately linearize the rates by using the first-order Taylor expansion, and then transform the resultant semi-infinite constraints into linear matrix inequalities (LMIs). The non-convex unit-modulus constraints of the reflection beamforming are handled by the penalized CCP [11]. 3) Numerical results confirm the effectiveness of

Manuscript received March 22, 2020; revised May 28, 2020; accepted June 1, 2020. Date of publication June 8, 2020; date of current version October 7, 2020. The work of Marco Di Renzo was supported by the European Commission through the H2020 ARIADNE Project under Grant 871464. The work of Arumugam Nallanathan was supported by under Grant EP/R006466/1. The associate editor coordinating the review of this article and approving it for publication was D. Tarchi. *(Corresponding author: Cunhua Pan.)*

Gui Zhou, Cunhua Pan, Hong Ren, and Arumugam Nallanathan are with the School of Electronic Engineering and Computer Science, Queen Mary University of London, London E1 4NS, U.K. (e-mail: g.zhou@qmul.ac.uk; c.pan@qmul.ac.uk; h.ren@qmul.ac.uk; a.nallanathang@qmul.ac.uk).

Kezhi Wang is with the Department of Computer and Information Sciences, Northumbria University, Newcastle upon Tyne NE1 8ST, U.K. (e-mail: kezhi.wang@northumbria.ac.uk).

Marco Di Renzo is with the Université Paris–Saclay, CNRS, CentraleSupélec, Laboratoire des Signaux et Systèmes, 91192 Gif-sur-Yvette, France (e-mail: marco.direnzo@centralesupelec.fr).

Digital Object Identifier 10.1109/LWC.2020.3000490

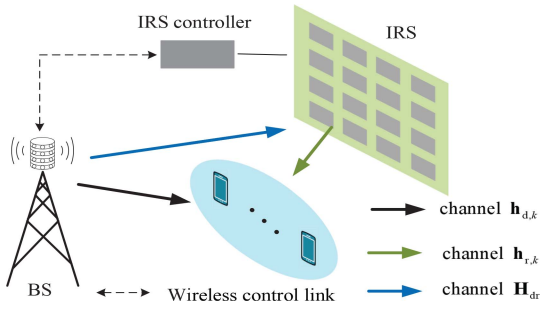

Fig. 1. An IRS-aided multiuser communication system.

the proposed algorithms in guaranteeing the QoS targets to all users.

II. System Model

A. Signal Transmission Model

We consider an IRS-aided MISO broadcast (BC) communication system shown in Fig. 1, in which there is a BS equipped with N transmit antennas serving K single-antenna users. Denote by $\mathbf{s} = [s_1, \ldots, s_K]^{\mathrm{T}} \in \mathbb{C}^{K\times 1}$ the Gaussian data symbols, in which each element is an independent random variable with zero mean and unit variance, i.e., $\mathbb{E}[\mathbf{s}\mathbf{s}^{\mathrm{H}}] = \mathbf{I}$. Denote by $\mathbf{F} = [\mathbf{f}_1, \ldots, \mathbf{f}_K] \in \mathbb{C}^{N\times K}$ the corresponding precoding vectors for the users. Then, the transmit signal at the BS is $\mathbf{x} = \mathbf{F}\mathbf{s}$ and the transmit power is $\mathbb{E}\{\mathrm{Tr}[\mathbf{x}\mathbf{x}^{\mathrm{H}}]\} = \|\mathbf{F}\|_F^2$.

In the MISO BC system, we propose to employ an IRS with the goal of enhancing the received signal strength of the users by reflecting signals from the BS to the users. It is assumed that the IRS has M passive reflection elements $\mathbf{e} = [e_1, \ldots, e_M]^{\mathrm{T}} \in \mathbb{C}^{M\times 1}$ and the modulus of each element is $|e_m|^2 = 1, 1 \le m \le M$. The reflection beamforming at the IRS is modeled as a diagonal matrix $\mathbf{E} = \iota \mathrm{diag}(\mathbf{e}) \in \mathbb{C}^{M\times M}$ where $\iota \in [0, 1]$ indicates the reflection efficiency. The channels from the BS to user k, from the BS to the IRS, and from the IRS to user k are denoted by $\mathbf{h}_{\mathrm{d},k} \in \mathbb{C}^{N\times 1}$, $\mathbf{H}_{\mathrm{dr}} \in \mathbb{C}^{M\times N}$, and $\mathbf{h}_{\mathrm{r},k} \in \mathbb{C}^{M\times 1}$, respectively.

The BS is responsible for designing the reflection beamforming at the IRS and sending it to the IRS controller [4]. Let us define the set of all users as $\mathcal{K} = \{1, 2, \ldots, K\}$, then the received signal of the users is

$$y_k = (\mathbf{h}_{\mathrm{d},k}^{\mathrm{H}} + \mathbf{h}_{\mathrm{r},k}^{\mathrm{H}}\mathbf{E}\mathbf{H}_{\mathrm{dr}})\mathbf{F}\mathbf{s} + n_k, \forall k \in \mathcal{K}, \tag{1}$$

where n_k is the received noise at user k, which is an additive white Gaussian noise (AWGN) with distribution $\mathcal{CN}(0, \sigma_k^2)$. The achievable data rate (bit/s/Hz) at user k is given by

$$R_k(\mathbf{F}, \mathbf{e}) = \log_2\left(1 + \left|(\mathbf{h}_{\mathrm{d},k}^{\mathrm{H}} + \mathbf{h}_{\mathrm{r},k}^{\mathrm{H}}\mathbf{E}\mathbf{H}_{\mathrm{dr}})\mathbf{f}_k\right|^2/\beta_k\right) \tag{2}$$

where $\beta_k = \|(\mathbf{h}_{\mathrm{d},k}^{\mathrm{H}} + \mathbf{h}_{\mathrm{r},k}^{\mathrm{H}}\mathbf{E}\mathbf{H}_{\mathrm{dr}})\mathbf{F}_{-k}\|_2^2 + \sigma_k^2, \forall k \in \mathcal{K}$ represents the interference-plus-noises (INs) term and $\mathbf{F}_{-k} = [\mathbf{f}_1, \ldots, \mathbf{f}_{k-1}, \mathbf{f}_{k+1}, \ldots, \mathbf{f}_K]$.

In an IRS-aided communication system, there are three types of channels: the direct channel from the BS to the user, i.e., $\mathbf{h}_{\mathrm{d},k}$, the indirect channel from the BS to the IRS, i.e., $\mathbf{H}_{\mathrm{dr}}$, and the reflection channel from the IRS to the user, i.e., $\mathbf{h}_{\mathrm{r},k}$. As mentioned in Section I, the reflection channel is more challenging to obtain than the other two channels. Hence, in this letter, we assume that the third type of channel is imperfect. The reflection channel $\{\mathbf{h}_{\mathrm{r},k}\}_{\forall k\in\mathcal{K}}$ can be modeled as $\{\mathbf{h}_{\mathrm{r},k} = \widehat{\mathbf{h}}_{\mathrm{r},k} + \mathbf{\Delta}_k\}_{\forall k\in\mathcal{K}}$, where $\{\widehat{\mathbf{h}}_{\mathrm{r},k}\}_{\forall k\in\mathcal{K}}$ denote the estimated channel vectors and $\{\mathbf{\Delta}_k\}_{\forall k\in\mathcal{K}}$ denote the corresponding channel error vectors. In this letter, we adopt a channel error bounded model, i.e., $\{\|\mathbf{\Delta}_k\|_2 \le \varepsilon_k\}_{\forall k\in\mathcal{K}}$, where ε_k is the radius of the uncertainty region known by the BS.

B. Problem Formulation

In the presence of imperfect CSI, we aim to minimize the total transmit power via the joint design of the precoding matrix $\mathbf{F}$ and the reflection vector $\mathbf{e}$ under worst-case QoS constraints, i.e., by ensuring that the achievable rate of each user is above a threshold for all possible channel error realizations. Mathematically, the worst-case robust design problem is formulated as

$$\min_{\mathbf{F},\mathbf{e}} \ \|\mathbf{F}\|_F^2 \tag{3a}$$

$$\text{s.t.} \ \ R_k(\mathbf{F}, \mathbf{e}) \ge r_k, \forall \|\mathbf{\Delta}_k\|_2 \le \varepsilon_k, \forall k \in \mathcal{K}, \tag{3b}$$

$$|e_m|^2 = 1, 1 \le m \le M. \tag{3c}$$

Constraints (3b) are the minimum QoS targets for each user, while constraints (3c) correspond to the unit-modulus requirements of the reflection elements at the IRS.

III. Robust Beamforming Design

Problem (3) is a non-convex problem and the main challenge lies in the non-convex QoS constraints (3b) over the CSI uncertainty regions and the non-convex unit-modulus constraints (3c). Since variables $\mathbf{F}$ and $\mathbf{e}$ are coupled, we propose an alternate optimization (AO) method to solve Problem (3).

A. Problem Transformation

To start with, the non-convexity of constraints (3b) can be addressed by firstly treating the INs $\boldsymbol{\beta} = [\beta_1, \ldots, \beta_K]^{\mathrm{T}}$ as auxiliary variables. Hence, constraints (3b) are rewritten as

$$\left|\left(\mathbf{h}_{\mathrm{d},k}^{\mathrm{H}} + \mathbf{h}_{\mathrm{r},k}^{\mathrm{H}}\mathbf{E}\mathbf{H}_{\mathrm{dr}}\right)\mathbf{f}_k\right|^2 \ge \beta_k(2^{r_k} - 1), \quad \forall \|\mathbf{\Delta}_k\|_2 \le \varepsilon_k, \forall k \in \mathcal{K}, \tag{4a}$$

$$\left\|\left(\mathbf{h}_{\mathrm{d},k}^{\mathrm{H}} + \mathbf{h}_{\mathrm{r},k}^{\mathrm{H}}\mathbf{E}\mathbf{H}_{\mathrm{dr}}\right)\mathbf{F}_{-k}\right\|_2^2 + \sigma_k^2 \le \beta_k, \quad \forall \|\mathbf{\Delta}_k\|_2 \le \varepsilon_k, \forall k \in \mathcal{K}. \tag{4b}$$

We first handle the infinite inequalities in (4a), which are non-convex. Specifically, the left hand side (LHS) of (4a) is approximated with a lower bound, as shown below.

Lemma 1: Let $\mathbf{f}_k^{(n)}$ and $\mathbf{E}^{(n)}$ be the optimal solutions obtained at iteration n, then a linear lower bound of $|(\mathbf{h}_{\mathrm{d},k}^{\mathrm{H}} + \mathbf{h}_{\mathrm{r},k}^{\mathrm{H}}\mathbf{E}\mathbf{H}_{\mathrm{dr}})\mathbf{f}_k|^2$ in (4a) at $(\mathbf{f}_k^{(n)}, \mathbf{E}^{(n)})$ is

$$\mathbf{h}_{\mathrm{r},k}^{\mathrm{H}}\mathbf{X}_k\mathbf{h}_{\mathrm{r},k} + \mathbf{h}_{\mathrm{r},k}^{\mathrm{H}}\mathbf{x}_k + \mathbf{x}_k^{\mathrm{H}}\mathbf{h}_{\mathrm{r},k} + c_k, \tag{5}$$

where

$$\mathbf{X}_k = \mathbf{E}\mathbf{H}_{\mathrm{dr}}\mathbf{f}_k\mathbf{f}_k^{\mathrm{H},(n)}\mathbf{H}_{\mathrm{dr}}^{\mathrm{H}}\mathbf{E}^{\mathrm{H},(n)} + \mathbf{E}^{(n)}\mathbf{H}_{\mathrm{dr}}\mathbf{f}_k^{(n)}\mathbf{f}_k^{\mathrm{H}}\mathbf{H}_{\mathrm{dr}}^{\mathrm{H}}\mathbf{E}^{\mathrm{H}} - \mathbf{E}^{(n)}\mathbf{H}_{\mathrm{dr}}\mathbf{f}_k^{(n)}\mathbf{f}_k^{\mathrm{H},(n)}\mathbf{H}_{\mathrm{dr}}^{\mathrm{H}}\mathbf{E}^{\mathrm{H},(n)},$$

$$\mathbf{x}_k = \mathbf{E}\mathbf{H}_{\mathrm{dr}}\mathbf{f}_k\mathbf{f}_k^{\mathrm{H},(n)}\mathbf{h}_{\mathrm{d},k} + \mathbf{E}^{(n)}\mathbf{H}_{\mathrm{dr}}\mathbf{f}_k^{(n)}\mathbf{f}_k^{\mathrm{H}}\mathbf{h}_{\mathrm{d},k} - \mathbf{E}^{(n)}\mathbf{H}_{\mathrm{dr}}\mathbf{f}_k^{(n)}\mathbf{f}_k^{\mathrm{H},(n)}\mathbf{h}_{\mathrm{d},k},$$
$$c_k = \mathbf{h}_{\mathrm{d},k}^{\mathrm{H}}(\mathbf{f}_k\mathbf{f}_k^{\mathrm{H},(n)} + \mathbf{f}_k^{(n)}\mathbf{f}_k^{\mathrm{H}} - \mathbf{f}_k^{(n)}\mathbf{f}_k^{\mathrm{H},(n)})\mathbf{h}_{\mathrm{d},k}.$$

Proof: Let a be a complex scalar variable. By applying Appendix B in [12], we have the inequality

$$|a|^2 \geq a^{*,(n)}a + a^* a^{(n)} - a^{*,(n)}a^{(n)} \tag{6}$$

for any fixed $a^{(n)}$. Then, (5) is obtained by replacing a and $a^{(n)}$ with $(\mathbf{h}_{\mathrm{d},k}^{\mathrm{H}} + \mathbf{h}_{\mathrm{r},k}^{\mathrm{H}}\mathbf{E}\mathbf{H}_{\mathrm{dr}})\mathbf{f}_k$ and $(\mathbf{h}_{\mathrm{d},k}^{\mathrm{H}} + \mathbf{h}_{\mathrm{r},k}^{\mathrm{H}}\mathbf{E}^{(n)}\mathbf{H}_{\mathrm{dr}})\mathbf{f}_k^{(n)}$, respectively. The proof is complete. ∎

With the aid of $\mathbf{h}_{\mathrm{r},k} = \widehat{\mathbf{h}}_{\mathrm{r},k} + \boldsymbol{\Delta}_k$ and Lemma 1, the inequality (4a) is reformulated as

$$\Delta\mathbf{h}_{\mathrm{r},k}^{\mathrm{H}}\mathbf{X}_k\Delta\mathbf{h}_{\mathrm{r},k} + 2\mathrm{Re}\Big\{(\mathbf{x}_k^{\mathrm{H}} + \widehat{\mathbf{h}}_{\mathrm{r},k}^{\mathrm{H}}\mathbf{X}_k)\Delta\mathbf{h}_{\mathrm{r},k}\Big\} + d_k \geq \beta_k(2^{r_k}-1), \forall\|\boldsymbol{\Delta}_k\|_2 \leq \varepsilon_k, \forall k \in \mathcal{K}, \tag{7}$$

where $d_k = \widehat{\mathbf{h}}_{\mathrm{r},k}^{\mathrm{H}}\mathbf{X}_k\widehat{\mathbf{h}}_{\mathrm{r},k} + \mathbf{x}_k^{\mathrm{H}}\widehat{\mathbf{h}}_{\mathrm{r},k} + \widehat{\mathbf{h}}_{\mathrm{r},k}^{\mathrm{H}}\mathbf{x}_k + c_k$.

In order to tackle the CSI uncertainties, the S-Procedure in [13] is used to transform (7) into equivalent LMIs as

$$\begin{bmatrix} \varpi_k\mathbf{I}_M + \mathbf{X}_k & (\mathbf{x}_k^{\mathrm{H}} + \widehat{\mathbf{h}}_{\mathrm{r},k}^{\mathrm{H}}\mathbf{X}_k)^{\mathrm{H}} \\ (\mathbf{x}_k^{\mathrm{H}} + \widehat{\mathbf{h}}_{\mathrm{r},k}^{\mathrm{H}}\mathbf{X}_k) & d_k - \beta_k(2^{r_k}-1) - \varpi_k\varepsilon_k^2 \end{bmatrix} \succeq \mathbf{0}, \quad \forall k \in \mathcal{K}, \tag{8}$$

where $\boldsymbol{\varpi} = [\varpi_1, \ldots, \varpi_K]^{\mathrm{T}} \geq 0$ are slack variables.

Now, we consider the uncertainties in $\{\boldsymbol{\Delta}_k\}_{\forall k\in\mathcal{K}}$ of (4b). To this end, we first adopt Schur's complement [14] to equivalently recast (4b) as

$$\begin{bmatrix} \beta_k - \sigma_k^2 & \mathbf{t}_k^{\mathrm{H}} \\ \mathbf{t}_k & \mathbf{I} \end{bmatrix} \succeq \mathbf{0}, \forall\|\boldsymbol{\Delta}_k\|_2 \leq \varepsilon_k, \forall k \in \mathcal{K}, \tag{9}$$

where $\mathbf{t}_k = ((\mathbf{h}_{\mathrm{d},k}^{\mathrm{H}} + \mathbf{h}_{\mathrm{r},k}^{\mathrm{H}}\mathbf{E}\mathbf{H}_{\mathrm{dr}})\mathbf{F}_{-k})^{\mathrm{H}}$.

Then, by using Nemirovski's lemma [15] and introducing the slack variables $\boldsymbol{\xi} = [\xi_1, \ldots, \xi_K]^{\mathrm{T}} \geq 0$, (9) is rewritten as

$$\begin{bmatrix} \beta_k - \sigma_k^2 - \xi_k & \widehat{\mathbf{t}}_k^{\mathrm{H}} & \mathbf{0}_{1\times M} \\ \widehat{\mathbf{t}}_k & \mathbf{I}_{(K-1)} & \varepsilon_k(\mathbf{E}\mathbf{H}_{\mathrm{dr}}\mathbf{F}_{-k})^{\mathrm{H}} \\ \mathbf{0}_{M\times 1} & \varepsilon_k\mathbf{E}\mathbf{H}_{\mathrm{dr}}\mathbf{F}_{-k} & \xi_k\mathbf{I}_M \end{bmatrix} \succeq \mathbf{0}, \quad \forall k \in \mathcal{K}, \tag{10}$$

where $\widehat{\mathbf{t}}_k = ((\mathbf{h}_{\mathrm{d},k}^{\mathrm{H}} + \widehat{\mathbf{h}}_{\mathrm{r},k}^{\mathrm{H}}\mathbf{E}\mathbf{H}_{\mathrm{dr}})\mathbf{F}_{-k})^{\mathrm{H}}$.

By using (8) and (10), we obtain the following approximated reformulation of Problem (3) as

$$\min_{\mathbf{F},\mathbf{e},\boldsymbol{\beta},\boldsymbol{\varpi},\boldsymbol{\xi}} \quad \|\mathbf{F}\|_F^2 \tag{11a}$$
$$\text{s.t.} \quad (8),\ (10),\ (3\text{c}), \tag{11b}$$
$$\boldsymbol{\varpi} \geq 0, \boldsymbol{\xi} \geq 0. \tag{11c}$$

It is difficult to optimize the variables $\mathbf{F}$ and $\mathbf{e}$ simultaneously as they are coupled in the LMIs (8) and (10). Therefore, the AO method is adopted to solve the subproblems corresponding to different sets of variables iteratively. Specifically, for a given reflection beamforming $\mathbf{e}$, the subproblem of Problem (11) corresponding to the precoder $\mathbf{F}$ is formulated as

$$\mathbf{F}^{(n+1)} = \arg\min_{\mathbf{F},\boldsymbol{\beta},\boldsymbol{\varpi},\boldsymbol{\xi}} \quad \|\mathbf{F}\|_F^2 \tag{12a}$$
$$\text{s.t.} \quad (8),\ (10),\ (11\text{c}), \tag{12b}$$

where $\mathbf{F}^{(n+1)}$ is the optimal solution obtained in the $(n+1)$-th iteration. Problem (12) is a semidefinite program (SDP) and can be solved by using the CVX tool.

On the other hand, for a given precoding matrix $\mathbf{F}$, the subproblem of Problem (11) corresponding to $\mathbf{e}$ is a feasibility-check problem. According to the Problem (P4') in [16], the converged solution of $\mathbf{e}$ can be improved by introducing slack variables $\mathbf{a} = [a_1, \ldots, a_K]^{\mathrm{T}}$ which are interpreted as the "signal-to-interference-plus-noise ratio (SINR) residual" of the users. Please refer to [16] for detailed information on the theory of "SINR residual". Thus, the feasibility-check problem of $\mathbf{e}$ is formulated as follows

$$\max_{\mathbf{e},\mathbf{a},\boldsymbol{\beta},\boldsymbol{\varpi},\boldsymbol{\xi}} \quad ||\mathbf{a}||_1 \tag{13a}$$
$$\text{s.t.} \quad \text{Modified}-(8), (10), (3\text{c}), (11\text{c}), \tag{13b}$$
$$\mathbf{a} \geq 0, \tag{13c}$$

where the Modified-(8) constraints are LMIs obtained from (8) by replacing $\beta_k(2^{r_k}-1)$ with $\beta_k(2^{r_k}-1) + a_k$ for $\forall k \in \mathcal{K}$.

However, the above problem cannot be solved directly due to the non-convex constraint (3c). In addition, the semidefinite relaxation (SDR) method used in [16] cannot always guarantee a feasible solution due to the fact that the QoS constraints may be violated when the SDR solution is not rank one. To handle this issue, we apply the penalty CCP [11] which is capable of finding a feasible solution that meets the unit-modulus constraint and the QoS constraints. In particular, the constraints $|e_m|^2 = 1, 1 \leq m \leq M$ can be equivalently rewritten as $1 \leq |e_m|^2 \leq 1, 1 \leq m \leq M$. The non-convex parts of these constraints are again linearized using $|e_m^{[t]}|^2 - 2\mathrm{Re}(e_m^{\mathrm{H}}e_m^{[t]}) \leq -1, 1 \leq m \leq M$ at fixed $e_m^{[t]}$. Following the penalty CCP framework, we impose the use of slack variables $\mathbf{b} = [b_1, \ldots, b_{2M}]^{\mathrm{T}}$ over the equivalent constraints of the unit-modulus constraints, which yields

$$\max_{\substack{\mathbf{e},\mathbf{a},\mathbf{b},\\ \boldsymbol{\beta},\boldsymbol{\varpi},\boldsymbol{\xi}}} \quad \|\mathbf{a}\|_1 - \lambda^{[t]}\|\mathbf{b}\|_1 \tag{14a}$$
$$\text{s.t.} \quad \text{Modified} - (8),\ (10),\ (11\text{c}),\ (13\text{c}), \tag{14b}$$
$$|e_m^{[t]}|^2 - 2\mathrm{Re}(e_m^{\mathrm{H}}e_m^{[t]}) \leq b_m - 1, 1 \leq m \leq M \tag{14c}$$
$$|e_m|^2 \leq 1 + b_{M+m}, 1 \leq m \leq M \tag{14d}$$
$$\mathbf{b} \geq 0, \tag{14e}$$

where $\lambda^{[t]}$ is the regularization factor to scale the impact of the penalty term $\|\mathbf{b}\|_1$, which controls the feasibility of the constraints. At low λ, Problem (14) targets to maximize the "SINR residual", while Problem (14) seeks for a feasible point rather than optimizing the "SINR residual" at high λ.

Problem (14) is an SDP and can be solved by using the CVX tool. The algorithm for finding a feasible solution of $\mathbf{e}$ is summarized in Algorithm 1. Some points are emphasized as follows: *a)* The maximum value λ_{max} is imposed to avoid numerical problems, that is, a feasible solution may not be found when the iteration converges under increasing large values of $\lambda^{[t]}$; *b)* The stopping criteria $\|\mathbf{b}\|_1 \leq \chi$ guarantees the unit-modulus constraints in the original Problem (13) to be met for a sufficiently low χ; *c)* The stopping criteria

Algorithm 1 Penalty CCP Optimization for Reflection Beamforming Optimization

Initialize: Initialize $\mathbf{e}^{[0]}$, $\gamma^{[0]} > 1$, and set $t = 0$.
1: **repeat**
2: **if** $t < T_{max}$ **then**
3: Update $\mathbf{e}^{[t+1]}$ from Problem (14);
4: $\lambda^{[t+1]} = \min\{\gamma\lambda^{[t]}, \lambda_{max}\}$;
5: $t = t + 1$;
6: **else**
7: Initialize with a new random $\mathbf{e}^{[0]}$, set $\gamma^{[0]} > 1$, and $t = 0$.
8: **end if**
9: **until** $\|\mathbf{b}\|_1 \leq \chi$ and $\|\mathbf{e}^{[t]} - \mathbf{e}^{[t-1]}\|_1 \leq \nu$.
10: Output $\mathbf{e}^{(n+1)} = \mathbf{e}^{[t]}$.

Algorithm 2 AO Algorithm for Problem (11)

Initialize: Initialize $\mathbf{e}^{(0)}$ and $\mathbf{F}^{(0)}$, and set $n = 0$.
1: **repeat**
2: Update $\mathbf{F}^{(n+1)}$ from Problem (12) with given $\mathbf{e}^{(n)}$;
3: Update $\mathbf{e}^{(n+1)}$ from Problem (13) with given $\mathbf{F}^{(n+1)}$;
4: $n \leftarrow n + 1$;
5: **until** The objective value $\|\mathbf{F}^{(n+1)}\|_F^2$ converges.

$\|\mathbf{e}^{[t]} - \mathbf{e}^{[t-1]}\|_1 \leq \nu$ controls the convergence of Algorithm 1; *d)* As mentioned in [11], a feasible solution for Problem (14) may not be feasible for Problem (13). Hence, the feasibility of Problem (13) is guaranteed by imposing a maximum number of iterations T_{max} and, if it is reached, the iteration is restarted based on a new initial point.

B. Algorithm Description

Algorithm 2 reports the AO method for solving Problem (11).

a) *Convergence analysis:* The convergence of Algorithm 2 can be guaranteed. In particular, denoting the objective value of Problem (12) as $F(\mathbf{F}, \mathbf{e})$, it follows that

$$F(\mathbf{F}^{(n)}, \mathbf{e}^{(n)}) \geq F(\mathbf{F}^{(n)}, \mathbf{e}^{(n+1)}) \geq F(\mathbf{F}^{(n+1)}, \mathbf{e}^{(n+1)}).$$

The above equality holds true because the objective value of Problem (12) is independent of $\mathbf{e}$, and also $\mathbf{e}^{(n+1)}$ is feasible for Problem (12) if it is a feasible solution for Problem (13). The above inequality follows from the globally optimal solution $\mathbf{F}^{(n+1)}$ of Problem (12) for a given $\mathbf{e}^{(n+1)}$. Hence, the sequence $\{F(\mathbf{F}^{(n)}, \mathbf{e}^{(n)})\}$ is non-increasing and the algorithm is guaranteed to converge.

b) *Initial point:* As for the method of initialization, $\mathbf{e}^{(0)}$ can be chosen as a full-1 vector for simplicity. Inspired by [17], the initial point $\mathbf{F}^{(0)}$ can be chosen as the optimal solution of the following optimization problem

$$\min_{\mathbf{F},\boldsymbol{\varphi}} \quad \sum_{k\in\mathcal{K}} (\varphi_k - 1)^2 \tag{15a}$$
$$\text{s.t.} \quad R_k(\mathbf{F}, \mathbf{e}) \geq \varphi_k \mathrm{r_k}, \forall k \in \mathcal{K} \tag{15b}$$
$$\varphi_k \geq 0, \forall k \in \mathcal{K}, \tag{15c}$$

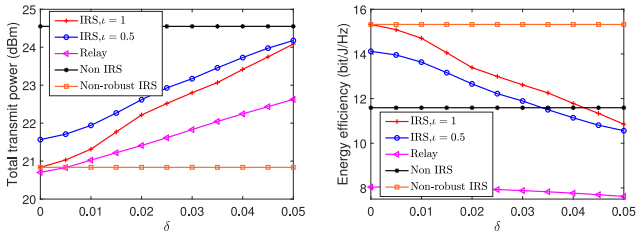

(a) The transmit power (b) The energy efficiency

Fig. 2. Performance versus the channel uncertainty level δ under $N = 6$, $M = 16$, $K = 4$ and $r = 4$ bit/s/Hz.

where $\boldsymbol{\varphi} = [\varphi_1, \ldots, \varphi_K]^{\mathrm{T}}$ is an auxiliary variable vector. Problem (15) is guaranteed to be feasible since at least $\{\varphi_k = 0, \forall k \in \mathcal{K}, \mathbf{F}^{(n)} = \mathbf{0}\}$ is a feasible solution. Problem (15) can also be solved by reformulating it into an alternative optimization problem that is similar to Problem (12). Denote by $\{\varphi_k^{(\mathrm{opt})}\}_{\forall k\in\mathcal{K}}$ the solution of Problem (15), then the corresponding optimal precoding matrix can be used as the initial point for Algorithm 2 if $\varphi_k^{(\mathrm{opt})} = 1, \forall k \in \mathcal{K}$.

IV. Numerical Results and Discussion

In this section, numerical results are provided to evaluate the performance of the proposed algorithm. We consider that the BS is equipped with $N = 6$ transmit antennas serving $K = 4$ users with the assistance of an IRS. The number of the reflection elements is $M = 16$. We assume a rectangular coordinate to discribe the system, i.e., the locations of the BS and IRS are (0 m, 0 m) and (50 m, 10 m) respectively, and users are distributed randomly on a circle centered at (70 m, 0 m) with radius 5 m.

The large-scale path loss is $\mathrm{PL} = -30 - 10\alpha \log_{10}(d)$ dB, where α is the path loss exponent and d is the link length in meters. The path loss exponents for the BS-IRS link, BS-user link, and the IRS-user link are equal to $\alpha_{\mathrm{BI}} = 2.2$ [18], $\alpha_{\mathrm{BU}} = 4$ and $\alpha_{\mathrm{IU}} = 2$, respectively. The small-scale fading of the channels $[\mathbf{H}_{\mathrm{dr}}, \{\mathbf{h}_{\mathrm{d},k}, \widehat{\mathbf{h}}_{\mathrm{r},k}\}_{\forall k\in\mathcal{K}}]$ follows a Rician distribution with Ricean factor 5. The line-of-sight (LoS) components are defined by the product of the steering vectors of the transmitter and receiver and the non-LoS components are drawn from a Rayleigh fading. The CSI error bounds are defined as $\varepsilon_k = \delta\|\widehat{\mathbf{h}}_{\mathrm{r},k}\|_2, \forall k \in \mathcal{K}$, where $\delta \in [0, 1)$ accounts for the relative amount of CSI uncertainties. The power of the AWGN at all users is set to -100 dBm and the target rates of all users are the same, i.e., $r_1 = \cdots = r_K = r$. The IRS and benchmark schemes considered are the following: 1) "IRS, $\iota = 1$(or 0.5)"; 2) "Non-robust IRS", in which the channel estimation error is ignored when designing the beamformings; 3) "Non IRS", in which there is no IRS in the MU-MISO system; 4) "Relay", in which a full-duplex relay is employed. The number of transmit (or receive) antennas at the relay is M.

Fig. 2 shows the total transmit power and energy efficiency versus the channel uncertainty level δ when $r = 4$ bit/s/Hz. It is observed from Fig. 2(a) that the required transmit power of the robust IRS beamforming scheme is higher than for other schemes. This is the price to pay to have a robust design and to employ passive reflection elements. In any case, it is less than

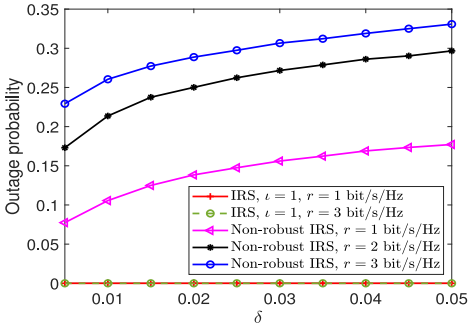

Fig. 3. Outage probability of rate versus the channel uncertainty level δ under $N = 6$, $M = 16$ and $K = 4$.

the "Non IRS" setup. The energy efficiency (EE) reported in Fig. 2(b) is defined as the ratio between the smallest achievable rate among the users and the total power consumption. The total power consumption of the IRS schemes is equal to $\|\mathbf{F}\|_F^2 + NP_{active} + MP_{passive}$ and that of the relay scheme is equal to $\|\mathbf{F}\|_F^2 + P_{relay} + (N + 2M)P_{active}$, where P_{relay} is the relay transmit power. We set the circuit power consumption of the active antennas to $P_{active} = 10$ mW and that of the passive antennas to $P_{active} = 5$ mW [19]. Fig. 2(b) illustrates the high EE performance of the IRS-aided systems compared with the relay system because of the low circuits power consumption of the passive elements in the IRS. In addition, from Fig. 2(a) and Fig. 2(b) we conclude that only if the reflection efficiency of the reflecting metasurfaces is high (ι is nearly 1) and the estimation error of the reflection channel is small (δ is less than 0.03), the IRS enhances the spectral and energy efficiency.

Fig. 3 shows the outage probability of the rate for the non-robust design. In particular, the outage probability is defined as the probability that the target rate of at least one user is not satisfied. It is observed that when the beamforming design ignores the channel error, the target rate of at least one user is frequently not met, especially for high values of r or δ. However, our adopted worst-case robust design method can guatantee no outage occurs.

V. Conclusion

In this letter, we considered the robust beamforming design for an IRS-aided MU-MISO system when the CSI is imperfect. The CSI uncertainties were addressed by using approximation and transformation techniques, and the non-convex unit-modulus constraints were solved under the penalty CCP framework. Numerical results demonstrated the robustness of our proposed algorithm.

References

[1] M. Di Renzo *et al.*, "Smart radio environments empowered by reconfigurable AI meta-surfaces: An idea whose time has come," *J. Wireless Commun. Netw.*, p. 129, 2019.

[2] M. Di Renzo *et al.*, "Reconfigurable intelligent surfaces vs. relaying: Differences, similarities, and performance comparison," 2019. [Online]. Available: https://arxiv.org/abs/1908.08747.

[3] E. Basar, M. Di Renzo, J. De Rosny, M. Debbah, M. Alouini, and R. Zhang, "Wireless communications through reconfigurable intelligent surfaces," *IEEE Access*, vol. 7, pp. 116753–116773, 2019.

[4] C. Pan *et al.*, "Intelligent reflecting surface aided MIMO broadcasting for simultaneous wireless information and power transfer," *IEEE J. Sel. Areas Commun.*, early access, Jun. 8, 2020, doi: 10.1109/JSAC.2020.3000802.

[5] X. Yu, D. Xu, and R. Schober, "Enabling secure wireless communications via intelligent reflecting surfaces," in *Proc. IEEE Global Commun. Conf. (GLOBECOM)*, Dec. 2019, pp. 1–6.

[6] G. Zhou, C. Pan, H. Ren, K. Wang, and A. Nallanathan, "Intelligent reflecting surface aided multigroup multicast MISO communication systems," *IEEE Trans. Signal Process.*, vol. 68, pp. 3236–3251, Apr. 2020. [Online]. Available: https://ieeexplore.ieee.org/document/9076830

[7] S. Zhang and R. Zhang, "Capacity characterization for intelligent reflecting surface aided MIMO communication," *IEEE J. Sel. Areas Commun.*, early access, Jun. 8, 2020, doi: 10.1109/JSAC.2020.3000814.

[8] T. Bai, C. Pan, Y. Deng, M. Elkashlan, and A. Nallanathan, "Latency minimization for intelligent reflecting surface aided mobile edge computing," *IEEE J. Sel. Areas Commun.*, to be published.

[9] H. Han, J. Zhao, D. Niyato, M. Di Renzo, and Q.-V. Pham, "Intelligent reflecting surface aided network: Power control for physical-layer broadcasting," 2019. [Online]. Available: https://arxiv.org/abs/1910.14383.

[10] M. Jung, W. Saad, Y. Jang, G. Kong, and S. Choi, "Performance analysis of large intelligent surfaces (LISs): Asymptotic data rate and channel hardening effects," *IEEE Trans. Wireless Commun.*, vol. 19, no. 3, pp. 2052–2065, Mar. 2020.

[11] T. Lipp and S. Boyd, "Variations and extension of the convex–concave procedure," *Optim. Eng.*, vol. 17, no. 2, pp. 263–287, 2016. [Online]. Available: https://doi.org/10.1007/s11081-015-9294-x

[12] C. Pan, H. Ren, M. Elkashlan, A. Nallanathan, and L. Hanzo, "Robust beamforming design for ultra-dense user-centric C-RAN in the face of realistic pilot contamination and limited feedback," 2018. [Online]. Available: https://arxiv.org/abs/1804.03990.

[13] Z.-Q. Luo, J. F. Sturm, and S. Zhang, "Multivariate nonnegative quadratic mappings," *SIAM J. Optim.*, vol. 14, no. 4, pp. 1140–1162, 2004.

[14] S. Boyd and L. Vandenberghe, *Convex Optimization*. Cambridge, U.K.: Cambridge Univ. Press, 2004.

[15] Y. C. Eldar, A. Ben-Tal, and A. Nemirovski, "Robust mean-squared error estimation in the presence of model uncertainties," *IEEE Trans. Signal Process.*, vol. 53, no. 1, pp. 168–181, Jan. 2005.

[16] Q. Wu and R. Zhang, "Intelligent reflecting surface enhanced wireless network via joint active and passive beamforming," *IEEE Trans. Wireless Commun.*, vol. 18, no. 11, pp. 5394–5409, Nov. 2019.

[17] C. Pan, H. Zhu, N. J. Gomes, and J. Wang, "Joint user selection and energy minimization for ultra-dense multi-channel C-RAN with incomplete CSI," *IEEE J. Sel. Areas Commun.*, vol. 35, no. 8, pp. 1809–1824, Aug. 2017.

[18] W. Tang *et al.*, "Wireless communications with reconfigurable intelligent surface: Path loss modeling and experimental measurement," 2019. [Online]. Available: https://arxiv.org/abs/1911.05326.

[19] E. Björnson, Ö. Özdogan, and E. G. Larsson, "Intelligent reflecting surface versus decode-and-forward: How large surfaces are needed to beat relaying?" *IEEE Wireless Commun. Lett.*, vol. 9, no. 2, pp. 244–248, Feb. 2020.